

Phonon-decoupled di-chromatic pumping scheme for highly efficient and indistinguishable single-photon sources

Luca Vannucci* and Niels Gregersen

DTU Electro, Department of Electrical and Photonics Engineering, 2800 Kongens Lyngby, Denmark

(Dated: September 19, 2022)

A key problem within single-photon sources engineering is to achieve population inversion of a quantum emitter on-demand and with the highest possible fidelity, without resorting to resonant laser pulses. A non-resonant pumping signal has the advantage of being separated in frequency from the single photons, but it typically triggers — or makes active use of — incoherent phonon-assisted scattering events, which preclude near unity fidelity in the population inversion and deteriorate the quality of the emitted photons. Here, we theoretically show that a coherent di-chromatic pumping scheme using short laser pulses and moderately large detuning effectively decouples the emitter from its phonon bath, allowing for population inversion arbitrarily close to unity. When considering a micropillar single-photon source driven with this scheme, we calculate very high photon emission into the cavity mode (0.953 photons per pulse), together with excellent indistinguishability (0.975). Such values are uniquely bounded by decoherence in the emission dynamics or practical considerations, and not by the excitation scheme.

Photonic quantum technologies [1, 2] — such as quantum computers, simulators and networks — require the availability of scalable and efficient sources of indistinguishable single photons [3]. The most successful single-photon source (SPS) is currently based on cavity-coupled semiconductor quantum dots (QDs) [4, 5], with a recent experiment reporting emission of single photons into a single-mode fiber with efficiency of 0.57 [6]. Using a carefully designed cavity, theoretical simulations predict an efficiency as high as 0.98, once the emitter is initialized in the excited state [7, 8]. An essential element is thus an efficient pumping scheme that prepares the desired initial state with the highest possible fidelity.

Initial experiments on SPSs relied on *p*-shell pumping [4, 9], whereby a laser pulse excites the QD into a higher energy state, which subsequently decays to the exciton level. Owing to the shorter wavelength of the pump with respect to the outgoing single photons, the laser is then removed via spectral filtering. However a high degree of photon indistinguishability is also required for a successful multi-photon interference [10, 11], and indistinguishability obtained under *p*-shell excitation is significantly reduced by the time-jitter effect [12]. Electrical triggering, which has been explored as an alternative to optical pumping [13, 14], suffers from a similar mechanism [15]. Resonant excitation with short laser pulses set a new milestone, enabling two-photon interference visibility ≥ 0.99 [4, 16]. A resonant scheme, however, requires cross-polarization filtering to distinguish the outgoing single photons from the pump. This, in turn, suppresses the number of collected photons by at least a factor 2, so that the total efficiency can never exceed 0.5.

A trade-off between these two competing effects is offered by near-resonant phonon-assisted excitation, where an efficiency of 0.50 has been demonstrated at the expense of a lower indistinguishability (0.91) [17]. Still, exciton preparation is limited to 0.85–0.90 fidelity both

in experiments and theory [17, 18], thus posing a fundamental limitation towards further increasing the efficiency. Promising strategies involving a periodic swing-up scheme [19, 20] or stimulated emission from the biexciton level [21–23] have been recently proposed. The former resulted in 0.97 population inversion estimated in experiments [20], while the latter has generated single photons with 0.93 indistinguishability and in-fiber efficiency of 0.51 [22]. It is thus natural to ask whether the figures of merit can be further increased towards unity. The answer to this question calls for a detailed analysis of the environment effects, as phonon-induced dissipation can always deteriorate the performance of the excitation scheme. This is however lacking in the above-mentioned cases, and an excitation scheme which is compatible with arbitrary increase towards unity of both efficiency and indistinguishability has not been demonstrated so far.

In this work, we show that a two-color (or di-chromatic) excitation scheme [24, 25] overcomes the limitations of the existing proposals, even when phonon-induced decoherence is fully taken into account. The two-color protocol makes use of two laser pulses symmetrically detuned from the QD emission frequency — that is, one on the blue side and one on the red side of the spectrum with respect to the emitter. Previous work has shown the possibility of partially populating the exciton level by acting on the relative pulse amplitudes [24, 25]. This effect is however significantly hindered by phonon scattering, with a population inversion ~ 0.6 predicted theoretically in Ref. [25]. Here, on the other hand, we solve this problem by showing how to remove phonon effects from the excitation process, and we uncover a phonon-decoupled regime where arbitrarily high population inversion is within reach for bulk QD in GaAs. We show that a state-of-the-art micropillar SPS driven with our scheme can generate up to 0.95 photons per pulse into the collection optics, together with excel-

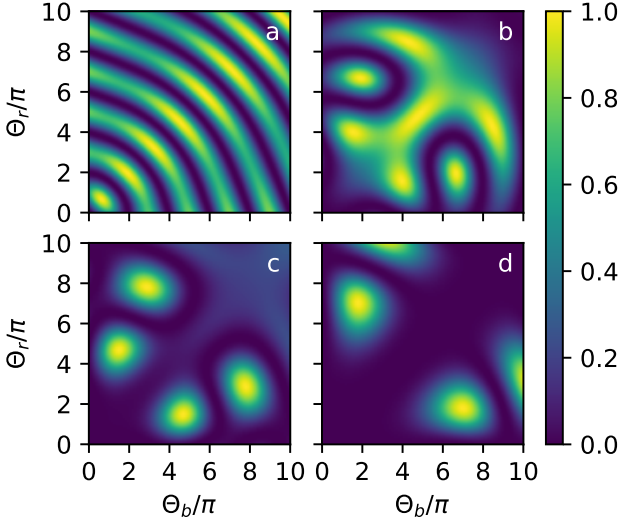


Figure 1. Exciton population in the absence of phonon coupling after the dichromatic laser pulse as a function of Θ_b and Θ_r , and for different values $\eta = 1$ (a), $\eta = 3$ (b), $\eta = 4$ (c), $\eta = 6$ (d).

lent indistinguishability which is on par with the resonant excitation scheme.

We begin by considering the dichromatic pumping dynamics of a QD in bulk in the absence of phonon coupling. We thus take a two-level system — ground state $|G\rangle$, excited state $|X\rangle$ — which is coupled to two laser pulses $\Omega_j(t)$, labeled with $j \in \{b, r\}$. The pulses are detuned in frequency by δ_j from the exciton frequency ω_X . They have Gaussian shape in the time domain, namely

$$\Omega_j(t) = \frac{\Theta_j}{t_p \sqrt{\pi}} e^{-\left(\frac{t}{t_p}\right)^2}, \quad (1)$$

where $\Theta_j = \int_{-\infty}^{+\infty} dt \Omega_j(t)$ is the pulse area, and t_p is the pulse temporal width. For simplicity, we assume identical width for both pulses and symmetric frequency detunings, i.e. $\delta_b = -\delta_r = \delta$. In a reference frame rotating at the exciton frequency ω_X , and making use of the rotating wave approximation, the system Hamiltonian reads

$$H_S(t) = \frac{\hbar}{2} [\Omega_b(t)e^{-i\delta t} + \Omega_r(t)e^{+i\delta t}] \sigma^\dagger + \text{h.c.}, \quad (2)$$

where $\sigma^\dagger = |X\rangle\langle G|$ is the QD raising operator [26]. The density operator ρ_S is readily obtained by solving the Von Neumann equation $\dot{\rho}_S(t) = -\frac{i}{\hbar} [H_S(t), \rho_S(t)]$, with the QD initialized in the ground state. For the moment, we neglect the QD spontaneous emission and any source of noise (e.g. charge and spin noise), to illustrate the physics of the pumping mechanism.

To assess the pumping efficiency, we consider as a figure of merit the excited state population $P_X(t) = \text{Tr} [\sigma^\dagger \sigma \rho_S(t)]$ at a time t after the pulse is gone (specifically, we use $t = 3t_p$). In the ideal scenario where any

source of decoherence and dissipation is neglected, P_X can take a maximum value of $P_X = 1$, corresponding to perfect population inversion. When the system dynamics is unitary and governed by Eq. (2), one can show that P_X after the laser pulse is determined by $f(\Theta_b, \Theta_r, \eta = t_p \delta)$, i.e. it depends on the product $\eta = t_p \delta$ and not on t_p and δ separately [26]. We explore such a functional dependence in Fig. 1. At $\eta = 1$ (Fig. 1a) we observe a periodic pattern that is reminiscent of Rabi oscillations, especially along the diagonal $\Theta_b = \Theta_r$. Indeed, the symmetric dichromatic driving with $\Omega_b(t) = \Omega_r(t) = \Omega(t)$ has a simple analytical solution $P_X = \sin^2(\xi)$, where $\xi = \int_{-\infty}^{+\infty} dt \Omega(t) \cos(\delta t)$ is the spectral component of the dichromatic laser pulse at the exciton frequency [25]. This shows that the oscillations along the diagonal are due to direct resonant coupling to the QD, which gives rise to the typical Rabi physics.

The spectral component of the driving laser at the exciton frequency, which scales as $e^{-\eta^2/4}$, becomes smaller when moving to larger values of η . Here, richer physics is observed in the exciton population. Rabi oscillations along the diagonal become progressively slower — one full oscillation is visible in Fig. 1b, while almost no oscillations are observed in Figs. 1c and 1d. At the same time, new bright spots exhibiting $P_X = 1$ emerge at $\Theta_b \neq \Theta_r$, symmetrically disposed with respect to the diagonal. They have nothing to do with direct resonant excitation, and are characteristic features of the dichromatic pumping scheme [25]. We notice that the distance of such sweet spots from the origin increases with increasing η . Such a distance is roughly linked to the total power provided by the laser pulse, which scales as $\sim (\Theta_b^2 + \Theta_r^2)/t_p$. Therefore, a trade-off between larger values of η — ensuring low spectral overlap of the laser pulse with the exciton frequency — and lower values to minimize the power is necessary. We choose here to work with $\eta = 6$, for which the laser spectral component at ω_X is $e^{-6^2/4} \approx 1 \cdot 10^{-4}$ relatively to its peak value.

We analyze now the performance of the dichromatic driving at $\eta = t_p \delta = 6$ in the presence of phonon-induced dissipation, focusing on the case of GaAs as host material. To this end, we adopt a master equation formalism within the weak-coupling approximation [27], whose implementation is detailed in Ref. [26]. The reduced density operator is determined by solving

$$\frac{d}{dt} \rho_S(t) = -\frac{i}{\hbar} [H_S(t), \rho_S(t)] + \mathcal{K}[\rho_S(t)] \quad (3)$$

where the extra term \mathcal{K} accounts for environment-induced effects. Due to the intrinsic asymmetry between phonon absorption and emission at low temperature, P_X is now function of t_p and δ separately. The behavior of P_X for $t_p = 6$ ps and $\delta = 1$ THz (corresponding to $\hbar \delta \approx 0.65$ meV) is reported in Fig. 2a. We observe that the features reported in Fig. 1d are significantly hindered by phonon scattering. For an excitation pulse predom-

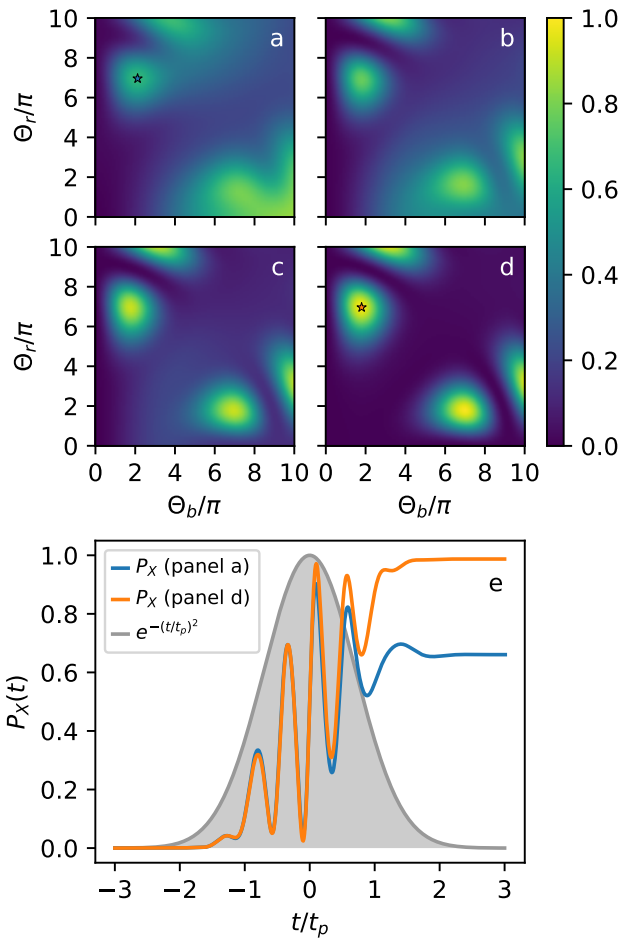


Figure 2. (a-d) Exciton population after the dichromatic laser pulse as a function of Θ_b and Θ_r , and for different values of t_p and δ . Here, the product $\eta = t_p\delta = 6$ is kept fixed, and phonon-induced effects are considered. Values are $\delta = 1$ THz (a), $\delta = 2$ THz (b), $\delta = 3$ THz (c), $\delta = 6$ THz (d). (e) Time evolution of $P_X(t)$ for the following configurations: $t_p = 6$ ps, $\delta = 1$ THz, $\Theta_b = 2.12\pi$, $\Theta_r = 6.96\pi$ (blue line); $t_p = 1$ ps, $\delta = 6$ THz, $\Theta_b = 1.80\pi$, $\Theta_r = 6.96\pi$ (orange line). See the corresponding markers in panels a and d.

inantly on the blue side (i.e. $\Theta_b > \Theta_r$), we observe a rather broad area revealing $P_X \approx 0.8$, which is attributed to phonon-assisted processes [17, 18]. On the other hand, the red side ($\Theta_b < \Theta_r$) shows an isolated peak similarly to the case without phonon coupling, but with a significantly smaller maximum value. We find $P_X = 0.661$ at $(\Theta_b, \Theta_r) = (2.12\pi, 6.96\pi)$, which is in qualitative agreement with Ref. [25], where a similar detuning have been used.

When moving to larger detuning (while simultaneously keeping $\eta = t_p\delta$ fixed), we observe that phonon scattering becomes progressively less detrimental. In Figs. 2b, 2c, and 2d, the dichromatic features gradually emerge from the background, with Fig. 2d begin almost identical to the corresponding calculation in the absence of phonons

(Fig. 1d). Indeed, at $\delta = 6$ THz ($\hbar\delta \approx 3.95$ meV) we find a maximum $P_X = 0.987$ at $(\Theta_b, \Theta_r) = (1.80\pi, 6.96\pi)$. It is possible to further increase P_X arbitrarily close to 1 by increasing the detuning beyond $\delta = 6$ ps at constant $\eta = t_p\delta$. For instance, we find $P_X = 0.999$ at $(t_p, \delta) = (0.2$ ps, 30 THz). However, a configuration with such ultra-short pulses in time is challenging to implement in the lab, and we will limit the discussion to the experimentally relevant range $t_p \in [1, 6]$ ps.

We interpret this result in terms of an effective phonon decoupling occurring at larger δ and shorter t_p . The population inversion is the result of a fast oscillating dynamics, which we illustrate in detail in Fig. 2e. Here, we report the evolution of P_X in time for the two configurations marked with a star in Figs. 2a and 2d. We observe that the excited state population oscillates on a time scale which is shorter than t_p . However, phonon relaxation occurs on a time scale of ~ 1 –5 ps [27]. For $(t_p, \delta) = (6$ ps, 1 THz) (corresponding to $P_X = 0.661$), the dynamics is sufficiently slow to allow for phonon-mediated relaxation events, and P_X remains well below 1 after the dichromatic pulse. For $(t_p, \delta) = (1$ ps, 6 THz) ($P_X = 0.987$), on the other hand, such oscillations occur on a time scale that is much shorter than the phonon dynamics. Phonons cannot follow the QD dynamics instantaneously and are effectively decoupled from the emitter, resulting in very little dissipation effect and much higher population inversion. At the same time, the phonon density of states is mostly contained within a range of 2–3 THz. When moving to $\delta = 6$ THz, the detuning becomes larger than the maximum phonon frequency and, as a consequence, no phonon states are available for phonon emission or absorption. This explains why the phonon-assisted events (which are particularly evident in the bottom right region of Fig. 2a) are no longer allowed at larger detuning.

The ability to capture the phonon decoupling effect numerically is crucial. Here, we have relied on the weak-coupling model because of its straightforward formulation and ease of implementation. In Ref. [26], we show that the weak-coupling master equation agrees very well with the more advanced TEMPO method [28, 29], which offers the benefit of being numerically exact at the cost of a larger numerical burden and coding complexity. The polaron master equation [30, 31], on the other hand, overestimates the effective phonon coupling at $t_p \sim 1$ ps. Therefore, it predicts a maximum performance of $P_X = 0.941$ for the optimal dichromatic scheme (instead of $P_X = 0.987$), which is a significant difference in the quest for a QD excitation scheme with near-unity efficiency.

Finally, we turn to the characterization of a state-of-the-art SPS driven with the dichromatic scheme presented above. Here, the relevant figures of merit are the number \mathcal{N} of single-photons collected into the collection optics per pulse, and their indistinguishability \mathcal{I} . State-of-the-art SPS rely on the cavity effect to funnel the emis-

sion into the zero-phonon line and direct the outgoing photons towards the collection optics. We thus introduce a single-mode cavity with annihilation operator a , which is assumed to be on resonance with the QD emission. In the rotating frame, the system Hamiltonian is now

$$H_S(t) = \left\{ \frac{\hbar}{2} [\Omega_b(t)e^{-i\delta t} + \Omega_r(t)e^{+i\delta t}] \sigma^\dagger + \text{h.c.} \right\} + \hbar g(a^\dagger \sigma + a \sigma^\dagger) \quad (4)$$

with g the QD-cavity coupling strength. We also add three Lindblad terms [32] to the master equation, which account for photon leakage out of the cavity at a rate κ , spontaneous decay of the QD into non-cavity (background) modes at a rate Γ_b , and pure dephasing at a rate γ_d induced by charge and nuclear spin fluctuations in the vicinity of the emitter. The master equation now reads

$$\frac{d}{dt} \rho_S = -\frac{i}{\hbar} [H_S(t), \rho_S] + \mathcal{K}[\rho_S] + \kappa \mathcal{L}_a[\rho_S] + \Gamma_b \mathcal{L}_\sigma[\rho_S] + \gamma_d \mathcal{L}_{\sigma^\dagger \sigma}[\rho_S] \quad (5)$$

with $\mathcal{L}_A[\rho] = A \rho A^\dagger - \frac{1}{2} \{ A^\dagger A, \rho \}$. As a prototypical cavity, we consider a micropillar device formed by sandwiching the QD between two stacks of DBR mirrors, whose performance has been optimized in previous work [7, 33]. Parameters for the microscopic modeling (g , κ , and Γ_b) are extracted from optical simulations of the electromagnetic environment, as described in Ref. [7]. We use here $g = 0.041$ THz, $\kappa = 0.46$ THz, $\Gamma_b = 0.45 \cdot 10^{-3}$ THz, and the dephasing rate is set at $\gamma_d = 0.13 \cdot 10^{-3}$ THz.

The number \mathcal{N} of single photons successfully reaching the collection optics is calculated as

$$\mathcal{N} = \gamma_{\text{coll}} \kappa \int_{t_0}^{+\infty} dt \langle a^\dagger(t) a(t) \rangle \quad (6)$$

where γ_{coll} is the collection efficiency, namely the fraction of photons emitted from the cavity that are successfully collected. We set this number to $\gamma_{\text{coll}} = 1$ for the dichromatic scheme. However, we will also consider the performance of a resonant excitation scheme, for which $\gamma_{\text{coll}} = 0.5$ due to the need for cross-polarization filtering. The indistinguishability of the emitted photons is determined as

$$\mathcal{I} = 1 - \frac{\int dt \int ds [G_{\text{pop}}^{(2)}(t, s) + g^{(2)}(t, s) - |g^{(1)}(t, s)|^2]}{\int dt \int ds [2G_{\text{pop}}^{(2)}(t, s) - |\langle a(t+s) \rangle \langle a^\dagger(t) \rangle|^2]} \quad (7)$$

with

$$G_{\text{pop}}^{(2)}(t, s) = \langle a^\dagger(t) a(t) \rangle \langle a^\dagger(t+s) a(t+s) \rangle \quad (8a)$$

$$g^{(2)}(t, s) = \langle a^\dagger(t) a^\dagger(t+s) a(t+s) a(t) \rangle \quad (8b)$$

$$g^{(1)}(t, s) = \langle a^\dagger(t) a(t+s) \rangle \quad (8c)$$

as detailed in Refs. [18, 34].

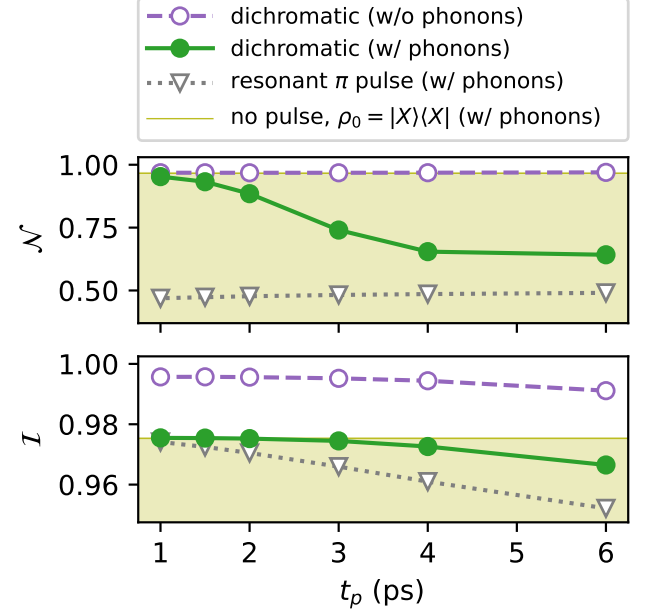


Figure 3. Collected photons \mathcal{N} and indistinguishability \mathcal{I} as a function of t_p for a dichromatic pumping scheme (with and without phonon coupling), and for a resonant π pulse of the same length in time (with phonon coupling). For each data point, the corresponding detuning for the dichromatic pulse is calculated as $\delta = 6/t_p$, while $\delta = 0$ for the resonant pulse. The upper bounds $\mathcal{N}^{(\text{UB})}$ and $\mathcal{I}^{(\text{UB})}$, obtained by initializing the system in $|X\rangle$, are also reported, and regions $\mathcal{N} \leq \mathcal{N}^{(\text{UB})}$ and $\mathcal{I} \leq \mathcal{I}^{(\text{UB})}$ are depicted as shaded areas.

Now, it must be noted that losses and decoherence may occur both during the *exciton preparation* phase and the *emission* phase. The former has been detailed in the preceding paragraphs. Regarding the latter, a nonzero value of Γ_b entails that some photons will be lost into background modes, resulting in a coupling efficiency to the cavity mode $\beta < 1$. This sets an upper bound on \mathcal{N} , which must satisfy $\mathcal{N} \leq \mathcal{N}^{(\text{UB})} = \beta$ for the case of pure single-photon emission [35]. Maximum performance is reached only in the ideal case where the system is artificially initialized in $|X\rangle$ at $t = t_0$, from which we obtain $\beta = 0.966$ for the specific cavity parameters used here. Similarly, indistinguishability is deteriorated both by temporal indeterminacy in the excited state preparation via the time-jitter effect [12], and by phonon scattering and noise-induced dephasing during the emission phase. Again, we calculate an upper bound $\mathcal{I}^{(\text{UB})}$ to \mathcal{I} by initializing the QD in the excited state, obtaining $\mathcal{I}^{(\text{UB})} = 0.975$. We emphasize that these hard limits are defined by dissipation and decoherence occurring *after* excitation, and not by imperfections in the excitation scheme.

In Fig. 3 we plot \mathcal{N} and \mathcal{I} for a dichromatic drive with $\eta = 6$ at different values of t_p , and we compare them with

the upper bounds $\mathcal{N}^{(\text{UB})}$ and $\mathcal{I}^{(\text{UB})}$. For each data point, the detuning $\delta = \eta/t_p$ is adjusted accordingly. For comparison, we also plot the performance of an SPS driven with a resonant π pulse of the same length t_p — for the latter, we thus use $\delta = 0$. The behavior of \mathcal{N} follows the pattern described previously, i.e. the best \mathcal{N} is obtained for shorter pulses, where the performance is almost at the same level as the one calculated in the absence of phonon coupling. Interestingly, all data points for dichromatic excitation are well above the 0.5 limit for resonant excitation, which is set by the need for polarization filtering. In particular, the value increases from $\mathcal{N} = 0.642$ at $t_p = 6 \text{ ps}$ to $\mathcal{N} = 0.953$ at $t_p = 1 \text{ ps}$. Importantly, we note that the deviation $1 - \mathcal{N} = 0.047$ is not a fundamental limitation of our scheme. Losses through spontaneous emission into background modes are calculated as $\mathcal{N}_b = \Gamma_b \int_{t_0}^{+\infty} dt \langle \sigma^\dagger(t) \sigma(t) \rangle = 0.034$ at $t_p = 1 \text{ ps}$. An additional loss $1 - P_X = 0.013$ is caused by imperfect exciton preparation $P_X = 0.987$, as obtained previously for a bulk QD in the absence of any emission mechanism, and we indeed observe that $\mathcal{N} + \mathcal{N}_b + (1 - P_X) = 1$. Note, however, that losses due to population inversion can be made arbitrarily small by resorting to shorter pulses, while background emission is unrelated to the pumping mechanism, and can be controlled using photonic engineering [8]. The indistinguishability \mathcal{I} , on the other hand, remains below the value calculated in the absence of phonons due to decoherence in the emission dynamics. Nevertheless, we obtain an excellent performance for any choice of parameters, with \mathcal{I} ranging from 0.966 at $t_p = 6 \text{ ps}$ up to 0.975 at $t_p = 1 \text{ ps}$ — the latter corresponding exactly to the upper bound due to unavoidable phonon-assisted events during the emission phase. It should be noted that the performance is better than the corresponding resonant excitation scheme for any value of t_p , with both schemes converging towards $\mathcal{I}^{(\text{UB})}$ at short t_p .

In conclusion, we have theoretically devised a new dichromatic pumping scheme which is capable of populating the exciton level of a semiconductor QD with arbitrary fidelity. This is obtained despite the presence of phonon coupling, and with a negligible spectral overlap of the laser pump with the QD transition frequency. Our proposal is appealing for the realization of scalable SPSs featuring simultaneous near-unity efficiency and indistinguishability. Calculations predict $\mathcal{N} = 0.953$ single photons collected per pulse with an indistinguishability $\mathcal{I} = 0.975$ for an optimal micropillar SPS device. Our proposed scheme allows further increasing these figures of merit arbitrarily towards unity by increasing the detuning of the laser pump and by photonic engineering of the background emission.

We thank Battulga Munkhbat for interesting discussions, and Martin A. Jacobsen for providing optical simulations of the micropillar SPS. This work is funded by the European Research Council (ERC-CoG "UNITY",

grant 865230) and by the Independent Research Fund Denmark (Grant No. DFF-9041-00046B).

* lucav@dtu.dk

- [1] Jeremy L. O'Brien, Akira Furusawa, and Jelena Vučković, "Photonic quantum technologies," *Nature Photonics* **3**, 687–695 (2009).
- [2] Jianwei Wang, Fabio Sciarrino, Anthony Laing, and Mark G. Thompson, "Integrated photonic quantum technologies," *Nature Photonics* **14**, 273–284 (2019).
- [3] Niels Gregersen, Dara P. S. McCutcheon, and Jesper Mørk, "Single-Photon Sources," in *Handbook of Optoelectronic Device Modeling and Simulation Vol. 2*, edited by Joachim Piprek (CRC Press, Boca Raton, 2017) Chap. 46, pp. 585–607.
- [4] N. Somaschi, V. Giesz, L. De Santis, J. C. Loredo, M. P. Almeida, G. Hornecker, S. L. Portalupi, T. Grange, C. Antón, J. Demory, C. Gómez, I. Sagnes, N. D. Lanzillotti-Kimura, A. Lemaître, A. Auffèves, A. G. White, L. Lanco, and P. Senellart, "Near-optimal single-photon sources in the solid state," *Nat. Photonics* **10**, 340–345 (2016).
- [5] Hui Wang, Hai Hu, T. H. Chung, Jian Qin, Xiaoxia Yang, J. P. Li, R. Z. Liu, H. S. Zhong, Y. M. He, Xing Ding, Y. H. Deng, Qing Dai, Y. H. Huo, Sven Höfling, Chao Yang Lu, and Jian Wei Pan, "On-Demand Semiconductor Source of Entangled Photons Which Simultaneously Has High Fidelity, Efficiency, and Indistinguishability," *Phys. Rev. Lett.* **122**, 113602 (2019).
- [6] Natasha Tomm, Alisa Javadi, Nadia O. Antoniadis, Daniel Najer, Matthias C. Löbl, Alexander R. Korsch, Rüdiger Schott, Sascha R. Valentin, Andreas D. Wieck, Arne Ludwig, and Richard J. Warburton, "A bright and fast source of coherent single photons," *Nat. Nanotechnol.* **16**, 399–403 (2021).
- [7] Bi-Ying Wang, Emil V. Denning, Uğur Meriç Gür, Chao-Yang Lu, and Niels Gregersen, "Micropillar single-photon source design for simultaneous near-unity efficiency and indistinguishability," *Phys. Rev. B* **102**, 125301 (2020).
- [8] Benedek Gaál, Luca Vannucci, Martin Arentoft Jacobsen, Julien Claudon, Jean-Michel Gérard, and Niels Gregersen, "Near-unity efficiency and photon indistinguishability for the "hourglass" single-photon source using suppression of background emission," [arXiv:2207.02035](https://arxiv.org/abs/2207.02035).
- [9] O. Gazzano, S. Michaelis de Vasconcellos, C. Arnold, A. Nowak, E. Galopin, I. Sagnes, L. Lanco, A. Lemaître, and P. Senellart, "Bright solid-state sources of indistinguishable single photons," *Nature Communications* **4**, 1425 (2013).
- [10] Jian-Wei Pan, Zeng-Bing Chen, Chao-Yang Lu, Harald Weinfurter, Anton Zeilinger, and Marek Żukowski, "Multiphoton entanglement and interferometry," *Rev. Mod. Phys.* **84**, 777–838 (2012).
- [11] Hui Wang, Jian Qin, Xing Ding, Ming-Cheng Chen, Si Chen, Xiang You, Yu-Ming He, Xiao Jiang, L. You, Z. Wang, C. Schneider, Jelmer J. Renema, Sven Höfling, Chao-Yang Lu, and Jian-Wei Pan, "Boson sampling with 20 input photons and a 60-mode interferometer in a 10^{14} -

dimensional hilbert space,” *Phys. Rev. Lett.* **123**, 250503 (2019).

[12] A. Kiraz, M. Atatüre, and A. Imamoglu, “Quantum-dot single-photon sources: Prospects for applications in linear optics quantum-information processing,” *Phys. Rev. A* **69**, 032305 (2004).

[13] Raj B. Patel, Anthony J. Bennett, Ken Cooper, Paola Atkinson, Christine A. Nicoll, David A. Ritchie, and Andrew J. Shields, “Quantum interference of electrically generated single photons from a quantum dot,” *Nanotechnology* **21**, 274011 (2010).

[14] A. Schlehahn, A. Thoma, P. Munnelly, M. Kamp, S. Höfling, T. Heindel, C. Schneider, and S. Reitzenstein, “An electrically driven cavity-enhanced source of indistinguishable photons with 61% overall efficiency,” *APL Photonics* **1**, 011301 (2016).

[15] P. Kaer, N. Gregersen, and J. Mork, “The role of phonon scattering in the indistinguishability of photons emitted from semiconductor cavity QED systems,” *New J. Phys.* **15**, 035027 (2013).

[16] Xing Ding, Yu He, Z.-C. Duan, Niels Gregersen, M.-C. Chen, S. Unsleber, S. Maier, Christian Schneider, Martin Kamp, Sven Höfling, Chao-Yang Lu, and Jian-Wei Pan, “On-demand single photons with high extraction efficiency and near-unity indistinguishability from a resonantly driven quantum dot in a micropillar,” *Phys. Rev. Lett.* **116**, 020401 (2016).

[17] S. E. Thomas, M. Billard, N. Coste, S. C. Wein, Priya, H. Ollivier, O. Krebs, L. Tazaïrt, A. Harouri, A. Lemaitre, I. Sagnes, C. Anton, L. Lanço, N. Somaschi, J. C. Loredo, and P. Senellart, “Bright polarized single-photon source based on a linear dipole,” *Phys. Rev. Lett.* **126**, 233601 (2021).

[18] Chris Gustin and Stephen Hughes, “Efficient pulse-excitation techniques for single photon sources from quantum dots in optical cavities,” *Advanced Quantum Technologies* **3**, 1900073 (2020).

[19] Thomas K. Bracht, Michael Cosacchi, Tim Seidelmann, Moritz Cygorek, Alexei Vagov, V. Martin Axt, Tobias Heindel, and Doris E. Reiter, “Swing-up of quantum emitter population using detuned pulses,” *PRX Quantum* **2**, 040354 (2021).

[20] Yusuf Karli, Florian Kappe, Vikas Remesh, Thomas K. Bracht, Julian Münzberg, Saimon Covre da Silva, Tim Seidelmann, Vollrath Martin Axt, Armando Rastelli, Doris E. Reiter, and Gregor Weihs, “Super scheme in action: Experimental demonstration of red-detuned excitation of a quantum emitter,” *Nano Lett.* **22**, 6567 (2022).

[21] Friedrich Sbresny, Lukas Hanschke, Eva Schöll, William Rauhaus, Bianca Scaparra, Katarina Boos, Eduardo Zubizarreta Casalengua, Hubert Riedl, Elena del Valle, Jonathan J. Finley, Klaus D. Jöns, and Kai Müller, “Stimulated generation of indistinguishable single photons from a quantum ladder system,” *Phys. Rev. Lett.* **128**, 093603 (2022).

[22] Yuming Wei, Shunfa Liu, Xueshi Li, Ying Yu, Xiangbin Su, Shulun Li, Xiangjun Shang, Hanqing Liu, Huiming Hao, Haiqiao Ni, Siyuan Yu, Zhichuan Niu, Jake Iles-Smith, Jin Liu, and Xuehua Wang, “Tailoring solid-state single-photon sources with stimulated emissions,” *Nat. Nanotechnol.* **17**, 470–476 (2022).

[23] Junyong Yan, Shunfa Liu, Xing Lin, Yongzheng Ye, Jiawang Yu, Lingfang Wang, Ying Yu, Yanhui Zhao, Yun Meng, Xiaolong Hu, Da-Wei Wang, Chaoyuan Jin, and Feng Liu, “Double-pulse generation of indistinguishable single photons with optically controlled polarization,” *Nano Lett.* **22**, 1483–1490 (2022).

[24] Yu-Ming He, Hui Wang, Can Wang, M. C. Chen, Xing Ding, Jian Qin, Z. C. Duan, Si Chen, J. P. Li, Run-Ze Liu, C. Schneider, Mete Atatüre, Sven Höfling, Chao-Yang Lu, and Jian-Wei Pan, “Coherently driving a single quantum two-level system with dichromatic laser pulses,” *Nature Physics* **15**, 941–946 (2019).

[25] Z. X. Koong, E. Scerri, M. Rambach, M. Cygorek, M. Brotons-Gisbert, R. Picard, Y. Ma, S. I. Park, J. D. Song, E. M. Gauger, and B. D. Gerardot, “Coherent dynamics in quantum emitters under dichromatic excitation,” *Phys. Rev. Lett.* **126**, 047403 (2021).

[26] See Supplemental Material for details on the system Hamiltonian and the QD-phonon interaction, some considerations on the functional dependence of P_X , the weak-coupling and polaron master equations, and their comparison with the TEMPO method.

[27] Ahsan Nazir and Dara P. S. McCutcheon, “Modelling exciton–phonon interactions in optically driven quantum dots,” *J. Phys.: Condens. Matter* **28**, 103002 (2016).

[28] A. Strathearn, P. Kirton, D. Kilda, J. Keeling, and B. W. Lovett, “Efficient non-markovian quantum dynamics using time-evolving matrix product operators,” *Nat. Commun.* **9**, 3322 (2018).

[29] The TEMPO collaboration, “OQuPy: A Python 3 package to efficiently compute non-Markovian open quantum systems.” (2020).

[30] Jake Iles-Smith, Dara P.S. McCutcheon, Ahsan Nazir, and Jesper Mørk, “Phonon scattering inhibits simultaneous near-unity efficiency and indistinguishability in semiconductor single-photon sources,” *Nat. Photonics* **11**, 521–526 (2017).

[31] Emil V. Denning, Jake Iles-Smith, Niels Gregersen, and Jesper Mørk, “Phonon effects in quantum dot single-photon sources,” *Opt. Mater. Express* **10**, 222–239 (2020).

[32] Heinz-Peter Breuer and Francesco Petruccione, *The theory of open quantum systems* (Oxford University Press, 2002).

[33] Bi-Ying Wang, Teppo Häyrynen, Luca Vannucci, Martin Arentoft Jacobsen, Chao-Yang Lu, and Niels Gregersen, “Suppression of background emission for efficient single-photon generation in micropillar cavities,” *Appl. Phys. Lett.* **118**, 114003 (2021).

[34] Chris Gustin and Stephen Hughes, “Pulsed excitation dynamics in quantum-dot–cavity systems: Limits to optimizing the fidelity of on-demand single-photon sources,” *Phys. Rev. B* **98**, 045309 (2018).

[35] \mathcal{N} can actually be larger than β if multi-photon emission occurs.

Supplemental Material to “Phonon-decoupled di-chromatic pumping scheme for highly efficient and indistinguishable single-photon sources”

Luca Vannucci* and Niels Gregersen

DTU Electro, Department of Electrical and Photonics Engineering, 2800 Kongens Lyngby, Denmark

(Dated: September 19, 2022)

I. METHODS

A. System Hamiltonian and phonon coupling

We consider a two-level system — ground state $|G\rangle$, excited state $|X\rangle$ — which is coupled to two laser pulses centered at angular frequencies ω_j , $j \in \{b, r\}$. Within the rotating wave approximation, the system Hamiltonian in the lab frame reads

$$H_S^{(0)}(t) = \hbar\omega_X |X\rangle\langle X| + \frac{\hbar}{2} \sum_{i=b,r} [\Omega_j(t)e^{-i\omega_j t}\sigma^\dagger + \Omega_j(t)e^{+i\omega_j t}\sigma] \quad (1)$$

where $\sigma = |G\rangle\langle X|$ is the QD lowering operator, and $\Omega_j(t)$ is the time-domain envelope of each pulse. In this work, we use an envelop with Gaussian shape,

$$\Omega_j(t) = \frac{\Theta_j}{t_p\sqrt{\pi}} e^{-\left(\frac{t}{t_p}\right)^2}, \quad (2)$$

where $\Theta_j = \int_0^{+\infty} dt \Omega_j(t)$ is the pulse area, and t_p is the pulse width in the time domain. For simplicity, we assume identical time width for both pulses.

The QD couples to a phonon environment — represented by $H_E = \sum_k \hbar\nu_k b_k^\dagger b_k$ — through the interaction Hamiltonian

$$H_I = \sum_k \hbar g_k (b_k^\dagger + b_k) |X\rangle\langle X|. \quad (3)$$

The environment is characterized by a phonon spectral density $J_{\text{ph}}(\omega) = \sum_k |g_k|^2 \delta(\omega - \nu_k) \approx \alpha\omega^3 e^{-\omega^2/\omega_c^2}$. For a QD in GaAs we use the coupling strength $\alpha = 0.03 \text{ ps}^2$, and the frequency cutoff $\omega_c = 2.2 \text{ THz}$ [1, 2]. The effect of the phonon bath is, among other things, to shift the exciton frequency to $\omega_X - D$, with (see e.g. Ref. [1])

$$D = \int_0^{+\infty} d\omega \frac{J_{\text{ph}}(\omega)}{\omega} = \frac{\sqrt{\pi}}{4} \alpha \omega_c^3. \quad (4)$$

It is convenient to move into a frame rotating at frequency $\omega_X - D$, where the system Hamiltonian reads

$$H_S(t) = -\hbar D |X\rangle\langle X| + \frac{\hbar}{2} \sum_{i=b,r} [\Omega_j(t)e^{-i\delta_j t}\sigma^\dagger + \Omega_j(t)e^{+i\delta_j t}\sigma], \quad (5)$$

with $\delta_j = \omega_j - \omega_X + D$ the frequency detuning of each pulse with respect to the re-normalized exciton frequency.

The dynamics in the absence of phonon coupling is readily obtained by setting $\alpha = 0$ (and thus $D = 0$).

B. Weak coupling master equation

We resort to the weak-coupling master equation to calculate the QD dynamics in the presence of phonon coupling [1]. The master equation for the density operator $\rho(t)$ reads

$$\frac{d}{dt}\rho(t) = -\frac{i}{\hbar}[H_S(t), \rho(t)] + \mathcal{K}(t)[\rho(t)] \quad (6)$$

where the phonon dissipation is given by

$$\mathcal{K}(t)[\rho(t)] = \int_0^{+\infty} ds C(s) [\hat{X}(t-s, t)\rho(t), X] + \text{h.c.} \quad (7)$$

with $X = \sigma^\dagger\sigma$, $\hat{X}(t-s, t) = U^\dagger(t-s, t)XU(t-s, t)$ and

$$U(t-s, t) = \mathcal{T} \exp \left[-\frac{i}{\hbar} \int_t^{t-s} du H_S(u) \right] \quad (8)$$

The environment correlation function reads

$$C(s) = \int_0^{+\infty} d\omega J_{\text{ph}}(\omega) \cdot \left[\coth \left(\frac{\hbar\omega}{2\kappa_B T} \right) \cos(\omega s) - i \sin(\omega s) \right] \quad (9)$$

with T the temperature, which is set at $T = 4 \text{ K}$ throughout this work.

The dynamics is obtained by solving the master equation via a 4th-order Runge-Kutta algorithm, with initial condition $\rho(t_0) = |G\rangle\langle G|$. We set $t_0 = -3t_p$ to make sure that $\Omega_j(t \leq t_0) \approx 0$. A second Runge-Kutta algorithm is used to calculate $U(t-s, t)$ in Eq. (8) by solving

$$\frac{d}{ds}U(t-s, t) = \frac{i}{\hbar}H_S(t-s)U(t-s, t) \quad (10)$$

at fixed t as a function of s , with initial condition $U(t-s, t)|_{s=0} = I$ (I being the identity). Finally, two-time correlation functions necessary for the indistinguishability calculation are evaluated using the quantum regression theorem [3].

* lucav@dtu.dk

C. Polaron theory

In the polaron theory, which is presented here for comparison, the Hamiltonian is diagonalized by applying the polaron transformation. This removes the QD-phonon interaction term [Eq. (3)] by applying a unitary displacement to the phonon modes [1]. The system dynamics is then obtained by solving the polaron master equation,

$$\frac{d}{dt}\rho(t) = -\frac{i}{\hbar}[H_S(t), \rho(t)] + \mathcal{K}_{\text{pol}}(t)[\rho(t)] \quad (11)$$

The system Hamiltonian, in a frame rotating at frequency $\omega_X - D$, is

$$H_S(t) = \frac{\hbar}{2}B \sum_{j=b,r} [\Omega_j(t)e^{-i\delta_j t}\sigma^\dagger + \Omega_j(t)e^{+i\delta_j t}\sigma], \quad (12)$$

Here the quantity $B = \exp[-\frac{1}{2}\phi(0)]$ is a phonon-induced re-normalization of the laser pulse amplitude, where $\phi(s)$ is the phonon correlation function

$$\phi(s) = \int_0^{+\infty} d\omega \frac{J_{\text{ph}}(\omega)}{\omega^2} \cdot \left[\coth\left(\frac{\hbar\omega}{2\kappa_B T}\right) \cos(\omega s) - i \sin(\omega s) \right] \quad (13)$$

Note that the polaron transformation automatically produces the frequency shift $\omega_X \rightarrow \omega_X - D$, which is thus not explicitly included in Eq. (12).

The second term in Eq. (11) is the polaron dissipator,

$$\mathcal{K}_{\text{pol}}[\rho(t)] = \frac{1}{\hbar^2} \int_0^{+\infty} ds \cdot \sum_{i=x,y} C_{ii}(s) [\hat{A}_i(t-s, t)\rho(t), A_i(t)] + \text{h.c.} \quad (14)$$

Here, the time dependent operators $A_i(t)$ are given by

$$A_x(t) = \frac{\hbar}{2}B \sum_{j=b,r} [\Omega_j(t)e^{-i\delta_j t}\sigma^\dagger + \Omega_j(t)e^{+i\delta_j t}\sigma], \quad (15)$$

$$A_y(t) = i\frac{\hbar}{2}B \sum_{j=b,r} [\Omega_j(t)e^{-i\delta_j t}\sigma^\dagger - \Omega_j(t)e^{+i\delta_j t}\sigma] \quad (16)$$

and $\hat{A}_i(t-s, t) = U^\dagger(t-s, t)A_i(t-s)U(t-s, t)$, with $U(t-s, t)$ as in Eq. (8). The environment correlation functions are

$$C_{xx}(s) = B^2 \{\cosh[\phi(s)] - 1\}, \quad (17)$$

$$C_{yy}(s) = B^2 \sinh[\phi(s)] \quad (18)$$

Again, we use a 4th-order Runge-Kutta algorithm to solve the polaron master equation, with initial condition $\rho(t_0 = -3t_p) = |G\rangle\langle G|$.

II. FUNCTIONAL DEPENDENCE OF P_X

Here we show that, for the case with no phonon coupling ($\alpha = 0$), the exciton population $P_X(t_1)$ after the laser pulse is a function of Θ_b , Θ_r , and $\eta = t_p\delta$. In the absence of phonons and any spontaneous decay, the dynamics is unitary and determined by $P_X(t_1) = |\langle X|U(t_1, t_0)|G\rangle|^2$ with

$$U(t_1, t_0) = \mathcal{T} \exp \left[-\frac{i}{\hbar} \int_{t_0}^{t_1} du H_S(u) \right]. \quad (19)$$

With a simple change of variable, the integral reads

$$\int_{t_0}^{t_1} du H_S(u) = \sum_j \frac{\hbar\Theta_j}{2\sqrt{\pi}} \int_{\frac{t_0}{t_p}}^{\frac{t_1}{t_p}} ds e^{-s^2} e^{-it_p\delta_j s} \sigma^\dagger + \text{h.c.} \quad (20)$$

Since $e^{-s^2} \approx 0$ for large $|s|$, one can safely extend the integration to $\pm\infty$ provided that t_0 and t_1 are chosen suitably. In practice, it is sufficient to take $t_0/t_p \leq -3$ and $t_1/t_p \geq +3$. With $\delta_b = -\delta_r = \delta$ one finally has

$$\begin{aligned} \int_{t_0}^{t_1} du H_S(u) &= \\ &= \frac{\hbar}{2\sqrt{\pi}} \int_{-\infty}^{+\infty} ds e^{-s^2} (\Theta_b e^{-i\eta s} + \Theta_r e^{+i\eta s}) \sigma^\dagger + \text{h.c.} \end{aligned} \quad (21)$$

which is indeed a function of Θ_b , Θ_r , and $\eta = t_p\delta$.

III. COMPARISON OF DIFFERENT METHODS

Predictions of the weak-coupling theory are compared with results obtained from the polaron master equation and the TEMPO method in Fig. 1. While being more computationally expensive, the TEMPO algorithm [4] is capable of returning numerically exact results. As such, it is a valuable tool to explore new physics in a non Markovian regime, or to assess the performance of approximate methods such as the weak-coupling and polaron theories. Here, TEMPO calculations are performed using the open source Python package *OQuPy* [5].

Figures 1a and 1b show the excited state population $P_X(t)$ predicted by the three methods for the optimal dichromatic configurations at $(t_p, \delta) = (6 \text{ ps}, 1 \text{ THz})$ and $(t_p, \delta) = (1 \text{ ps}, 6 \text{ THz})$, which are respectively marked with a blue and an orange star in Fig. 2 of the main text. The weak-coupling prediction is in perfect quantitative agreement with the TEMPO calculation, both for slower and faster driving. This certifies that the weak-coupling master equation is indeed sufficient to accurately describe the pumping dynamics even in the presence of fast oscillations, provided that the phonon coupling is not too strong and the temperature is sufficiently low. On the other hand, we observe a deviation of the polaron results

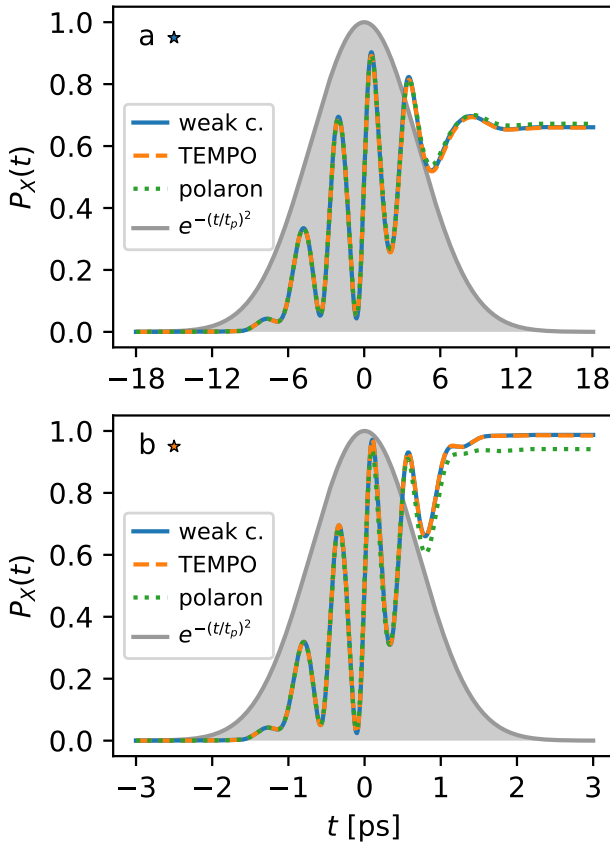


Figure 1. Comparison of the time evolution $P_X(t)$ predicted by the weak-coupling master equation, the polaron master equation, and the TEMPO algorithm. Parameters are: $t_p = 6$ ps, $\delta = 1$ THz, $\Theta_b = 2.12\pi$, $\Theta_r = 6.96\pi$ (panel a); $t_p = 1$ ps, $\delta = 6$ THz, $\Theta_b = 1.80\pi$, $\Theta_r = 6.96\pi$ (panel b). See corresponding markers in Fig. 2a and 2d of the main text.

from the other two lines. For the case of fast driving ($t_p = 1$ ps, Fig. 1b), we obtain $P_X^{(\text{pol})} = 0.941$, in contrast with $P_X^{(\text{pol})} = 0.987$ obtained earlier. Thus, while being in qualitative agreement with the other two methods, the polaron underestimates the final probability by a factor $\sim 5\%$, which is a significant deviation in the quest for a perfect SPS performance. The reason is that the polaron theory overestimates phonon-induced dissipation when the exciton population oscillates too fast, i.e. on a time scale that is shorter than the phonon relaxation time — a very relevant case in this work.

[1] Ahsan Nazir and Dara P. S. McCutcheon, “Modelling exciton–phonon interactions in optically driven quantum dots,” *J. Phys.: Condens. Matter* **28**, 103002 (2016).

[2] Emil V. Denning, Jake Iles-Smith, Niels Gregersen, and Jesper Mørk, “Phonon effects in quantum dot single-photon sources,” *Opt. Mater. Express* **10**, 222–239 (2020).

[3] Heinz-Peter Breuer and Francesco Petruccione, *The theory of open quantum systems* (Oxford University Press, 2002).

[4] A. Strathearn, P. Kirton, D. Kilda, J. Keeling, and B. W. Lovett, “Efficient non-markovian quantum dynamics using time-evolving matrix product operators,” *Nat Commun* **9**, 3322 (2018).

[5] The TEMPO collaboration, “OQuPy: A Python 3 package to efficiently compute non-Markovian open quantum systems.” (2020).